

# LCGC

## north america

solutions for separation scientists

Volume 34 Number 10 October 2016  
[www.chromatographyonline.com](http://www.chromatographyonline.com)

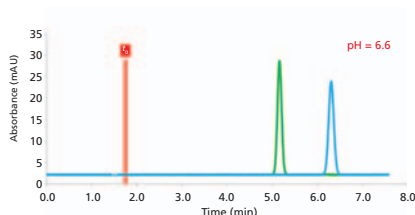
### An Interactive System for Comparing Reversed-Phase LC Columns

### Troubleshooting Ghost Peaks in Gradient LC

### Quality Control for Pharmaceutical Salts

### A Free Spreadsheet-Based Program for Learning and Teaching LC

# HPLC Teaching Assistant: A New Tool for Learning and Teaching Liquid Chromatography, Part I



The free spreadsheet-based program HPLC Teaching Assistant was developed for effective and innovative learning and teaching of liquid chromatography. This software allows teachers to illustrate the basic principles of high performance liquid chromatography (HPLC) using virtual chromatograms (simulated chromatograms) obtained under various analytical conditions. In the first installment of this series, we demonstrate the possibilities offered by this spreadsheet to illustrate the concept of chromatographic resolution, including the impact of retention, selectivity, and efficiency; understand the plate height (van Deemter) equation and kinetic performance in HPLC; recognize the importance of analyte lipophilicity ( $\log P$ ) on retention and selectivity in reversed-phase HPLC mode; and manipulate or adapt reversed-phase HPLC retention, taking into account the acido-basic properties ( $pK_a$ ) of compounds and the mobile-phase pH.

High performance liquid chromatography (HPLC) remains one of the most widely used analytical techniques in industry and is taught at universities in analytical chemistry programs. Because HPLC separation is based on the partitioning of a solute between a mobile phase and a stationary phase, the technique is particularly difficult to master. There are a significant number of parameters (for example, physicochemical properties and molecular weight of the solutes; nature, composition, temperature, pH, and flow rate of the mobile phase; and chemical nature and dimensions of the stationary phase) that can influence the quality of the separation (retention time, selectivity, efficiency, pressure drop, peak area).

Several commercial HPLC simulators are available on the market, including Drylab (Molnar-Institute) (1), Chromsword (Iris Tech) (2), LC & GC Simulator (Advanced Chemistry Development) and Osiris (Datlys) (3). These simulators are particularly useful for efficiently developing HPLC methods based on a limited number of initial experiments and can also be used to

better understand the principles of HPLC. However, these simulators remain difficult to use and expensive to purchase.

To easily understand the principles of chromatography in a relatively inexpensive way, some free or low-cost computer-based HPLC simulators have also been proposed (4–7). As reported by Boswell and colleagues (8), there are currently six HPLC simulators, but most are not available anymore or are not fully compatible with modern computers. To the best of our knowledge, the most interesting HPLC simulator was released in 2013 and is free (8). The software interface is relatively easy to use and produces a simulated chromatogram that is redrawn when the experimental parameters are changed.

In comparison to this software, the philosophy of our program, entitled “HPLC Teaching Assistant,” is different but complementary. First, our program is a spreadsheet that can be easily used on any computer without the need to install a Java environment. Second, our spreadsheet allows making links between compounds’ physicochemical properties (partitioning coefficient,  $pK_a$ ) and chromatographic behavior.

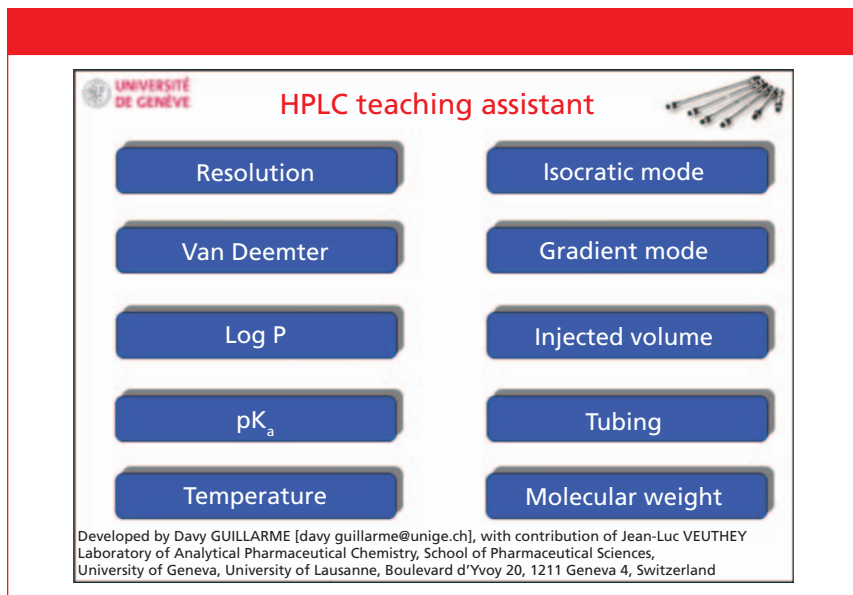


**Figure 1:** Main menu of HPLC Teaching Assistant.

Last but not least, each spreadsheet of our calculator provides an understanding of a single concept (for example, the effect of the mobile-phase pH on the chromatographic behavior). This series of two articles provides the theoretical background of the spreadsheet and gives some practical exam-

ples to illustrate the usefulness of this tool (see Figure 1).

### Understanding the Concept of Chromatographic Resolution Theoretical Background

In liquid chromatography (LC), the separa-

tion of two peaks is described by their resolution ( $R_s$ ), which represents the difference in retention times ( $t_{R}$ ) divided by the average peak widths at baseline ( $W$ ), according to the following equation:

$$R_s = \frac{2 \times (t_{R2} - t_{R1})}{W_1 + W_2} \quad [1]$$

To better understand the impact of analytical conditions on the overall resolution, the fundamental equation of resolution can be used to interpret the chromatograms obtained during method development.  $R_s$  can also be expressed based on the retention factor ( $k$ ), selectivity ( $\alpha$ ), and plate number ( $N$ ):

$$R_s = \frac{\sqrt{N}}{4} \times \frac{k}{k+1} \times \frac{\alpha-1}{\alpha} \quad [2]$$

### Using the “Resolution” Spreadsheet

In the first spreadsheet, entitled “resolution,” the impact of  $k$ ,  $\alpha$ , and  $N$  on  $R_s$  can be directly visualized. For this purpose, a chromatogram was simulated to show the chromatographic resolution of two molecules when modifying  $k$ ,  $\alpha$ , and  $N$ . For this example, the column had a void time of



## Pesticide Residues Analysis Webinar Shifting the Paradigm in GC-MS Pesticide Analysis

**ON-DEMAND WEBCAST** Aired September 8, 2016

Register free at: [www.chromatographyonline.com/lcgc/paradigm](http://www.chromatographyonline.com/lcgc/paradigm)

### All attendees will receive a free executive summary of this webcast!

There is growing interest in the use of gas chromatography–high resolution accurate mass (HRAM) mass spectrometry for the non-targeted screening of pesticides in food. This approach is now enabled by the improved full scan performance of the latest GC-HRAM systems. It is now possible to analyze targeted, suspected, and unexpected residues in a single workflow with an easy-to-use GC-MS system that provides an unprecedented level of performance in routine analysis.

Join Prof. Fernandez-Alba, who will share his thoughts on the performance of GC-HRAM technology including the ease of use, performance, and effectiveness of the GC-MS system and intelligent software for the analysis of pesticides in fruit and vegetables.

### Who Should Attend

- Scientists who need simultaneous targeted and non-targeted analysis in the same run
- Scientists working in routine laboratories who need robust quantitative performance of GC-QqQ, but with the increased selectivity of HRAM
- Scientists who want to gain a broader, deeper understanding of their samples

For questions, contact Kristen Moore at [kristen.moore@ubm.com](mailto:kristen.moore@ubm.com)

### PRESENTER

**Prof. Amadeo R. Fernández-Alba**  
Professor, Analytical Chemistry,  
University of Almeria, Spain  
Head, European Reference Laboratory for  
Pesticide Residues in Fruits and Vegetables

*Moderator:*

**Laura Bush**, Editorial Director, LCGC

### Key Learning Objectives

- Simplicity and ease of GC-HRAM acquisition, data processing and spectral matching
- Importance of high resolving power and sub-ppm mass accuracy for selectivity
- Compliance of HRAM data with SANTE/11945/2015 Guidelines

Sponsored by

**thermo**  
scientific

Presented by

**LCGC**



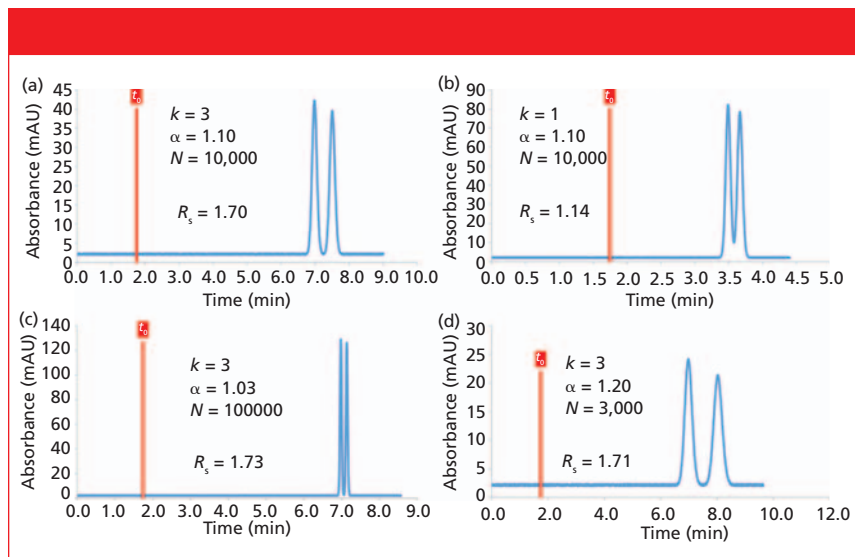


**Figure 2:** Simulated chromatograms to better understand the impact of retention, selectivity, and efficiency on the overall resolution.

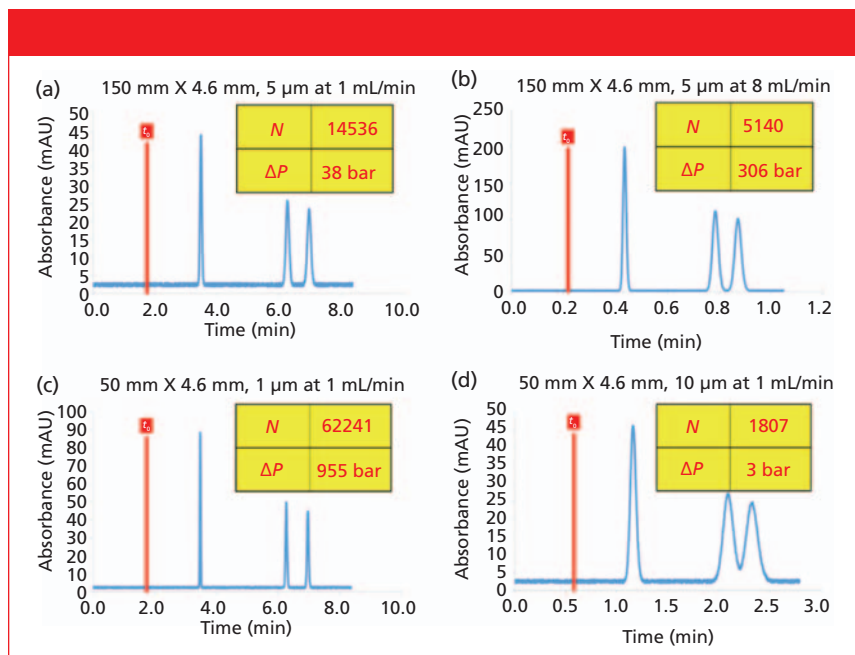


**Figure 3:** Simulated chromatograms to illustrate the impact of the column dimensions (length and particle size) and mobile-phase flow rate on the efficiency and column back pressure.

1.74 min (corresponding to a 150 mm  $\times$  4.6 mm column operated at 1 mL/min).

In addition to the simulated chromatogram, three graphics at the bottom of the spreadsheet illustrate the change in resolution with the three individual variables, namely,  $k$ ,  $\alpha$ , and  $N$ . The impact of  $\alpha$  on the resolution is strong: For  $\alpha$  values between 1 and 4, the resolution drastically increases, and a plateau is only attained for very high (inaccessible)  $\alpha$  values ( $\alpha > 4$ ). The retention factor also has a significant impact on resolution for low  $k$  values, but

its impact becomes moderate for  $k$  between 3 and 10 and low for  $k$  higher than 10. For  $k > 10$ , the analysis time becomes long, and the improvement in the resolution is minor (this can be easily verified by simulating a chromatogram obtained under conditions of very high  $k$  values). Finally, because efficiency is expressed as the square root in the resolution equation, its impact on resolution is moderate to low, and  $N$  must be dramatically increased to significantly improve  $R_s$ .

From this spreadsheet, four different conditions were simulated to better illustrate the

influence of  $k$ ,  $\alpha$ , and  $N$  on  $R_s$ , as shown in Figure 2. In Figure 2a, the selectivity, retention factor, and efficiency were reasonable, leading to an overall resolution of 1.70. Figure 2b illustrates the conditions of an insufficient retention factor in LC ( $k = 1$ ), thereby leading to a significant reduction in resolution ( $R_s = 1.14$ ). Figure 2c shows that a very low selectivity ( $\alpha = 1.03$ ) can be compensated by a very high plate number ( $N = 100,000$  plates). Finally, Figure 2d proves that selectivity is the primary driver for optimizing chromatographic separation in LC. As shown on this simulated chromatogram, when the selectivity is appropriate ( $\alpha = 1.20$ ), there is no need for a very high plate count (only 3000 plates in this case).

Based on these observations, it is easy to understand why method development follows three successive steps after selecting the appropriate stationary and mobile-phase conditions:

- Select a column with a sufficient plate number considering the complexity of the sample to be analyzed (usually a column generating 10,000 plates is a good starting point).
- Adjust the solvent strength to have a reasonable retention factor ( $k$  between 2 and 10).
- Optimize selectivity by tuning different chromatographic parameters.

## Understanding the Kinetic Performance and van Deemter Curves

### Theoretical Background

In LC, the column dimensions (length, internal diameter, and particle size), as well as the mobile-phase flow rate and viscosity, have an impact on the plate number ( $N$ ) and column back pressure ( $\Delta P$ ). In the second spreadsheet, the kinetic performance is shown for a mixture of three compounds with a molecular weight of approximately 100 g/mol. All the calculations were made for a column with a total porosity ( $\epsilon$ ) of 0.7 and a flow resistance ( $\Phi$ ) of 500. The column temperature was 30 °C, and the mobile phase was a mixture of 30% acetonitrile and 70% aqueous buffer.

To calculate the plate number ( $N$ ) based on the column dimensions, the following equation was used:

$$N = \frac{L}{H} \quad [3]$$

where  $L$  is the column length (in millime-

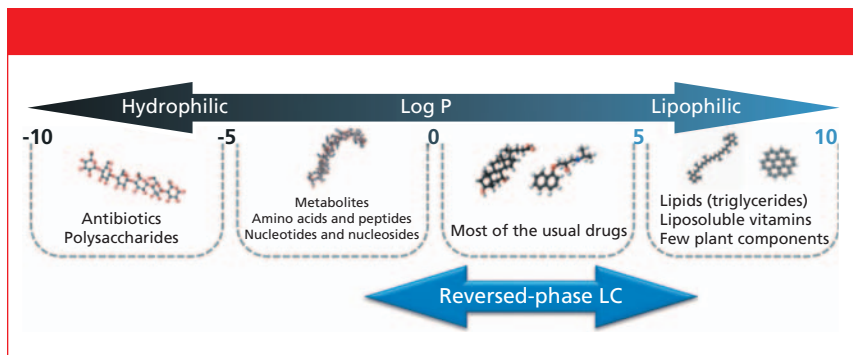


**Figure 4:** Log  $P$  values of common substances and applicability of the reversed-phase LC mode.

ters) and  $H$  is the height equivalent to a theoretical plate (in micrometers). To estimate the  $H$  value, the van Deemter equation was considered:

$$H = A + \frac{B}{u} + Cu \quad [4]$$

In this equation,  $A$ ,  $B$ , and  $C$  correspond to eddy dispersion, longitudinal diffusion, and mass transfer, respectively. They represent a different set of constants for a particular solute, column, and mobile-phase conditions. The  $u$  value is the linear velocity, which is related to the mobile-phase flow rate ( $F$ ), column porosity ( $\epsilon$ ),

and column internal diameter ( $d_c$ ) using the following relationship:

$$u = \frac{4 \times F}{\pi \times d_c^2 \times \epsilon} \quad [5]$$

To use generic  $a$ ,  $b$ , and  $c$  terms ( $a = 1$ ,  $b = 4$ ,  $c = 0.05$  in our case), which are independent on the analytical conditions, the van Deemter equation was transformed into its reduced form:

$$h = a + \frac{b}{v} + cv \quad [6]$$

where  $h$  is the reduced height equivalent to a theoretical plate and  $v$  is the reduced linear

velocity. The following two equations provide the definitions for these two reduced parameters.

$$h = \frac{H}{d_p} \quad [7]$$

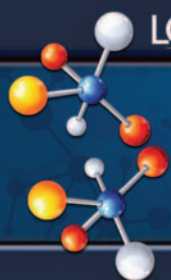
$$v = \frac{u \times d_p}{D_m} \quad [8]$$

Here,  $d_p$  represents the column particle diameter (in micrometers) and  $D_m$  is the diffusion coefficient of the solute in the mobile phase, which can be estimated using the Wilke-Chang equation (9).

Finally, the column pressure drop was calculated using Darcy's law, with  $\eta$  being the mobile-phase viscosity:

$$\Delta P = \frac{\eta \times L \times u \times \Phi}{d_p^2} \quad [9]$$

In the spreadsheet entitled "Efficiency," the impact of the column dimensions ( $L_{col}$ ,  $d_{col}$ , and  $d_p$ ) and the mobile-phase flow rate ( $F$ ) on  $N$  and  $\Delta P$  can be directly visualized. A simulated chromatogram with three compounds ( $k = 1.0, 2.6,$  and  $3.0$ ) shows the corresponding chromatogram when modifying the column dimensions and flow rate. In addition, the van Deemter curve,  $H = f(u)$ ,



LC/GC EDITORS' SERIES

# Advancing Chiral Separations

ON-DEMAND WEBCAST

Register for free at [www.chromatographyonline.com/lcgc/chiral](http://www.chromatographyonline.com/lcgc/chiral)

## Event Overview:

As the number and complexity of chiral drugs and biologically active compounds increases, there is a growing need to advance chiral separation techniques. The number one way to separate chiral compounds is with HPLC using chiral stationary phases. This editorial web seminar presented by Zachary S. Breitbach of AbbVie, will address the need for improved chiral separations and discuss approaches for screening chiral columns, as well as new advancements in chiral column technology that lead to high efficiency and ultrafast chiral separations.

For questions, contact Ethan Castillo at [ethan.castillo@ubm.com](mailto:ethan.castillo@ubm.com)



### Presenter

ZACHARY BREITBACH, Ph.D.  
Senior Scientist II  
AbbVie



### Moderator

LAURA BUSH  
Editorial Director  
LC/GC

## Key Learning Objectives:

- A brief background of HPLC chiral separations and the state of the art
- High throughput and SFC chiral screening
- High efficiency and high speed chiral separations
- Instrumental considerations for improved chiral separations

## Who Should Attend:

- Anyone interested in using or currently using chiral separations
- HPLC and SFC users

Sponsored by



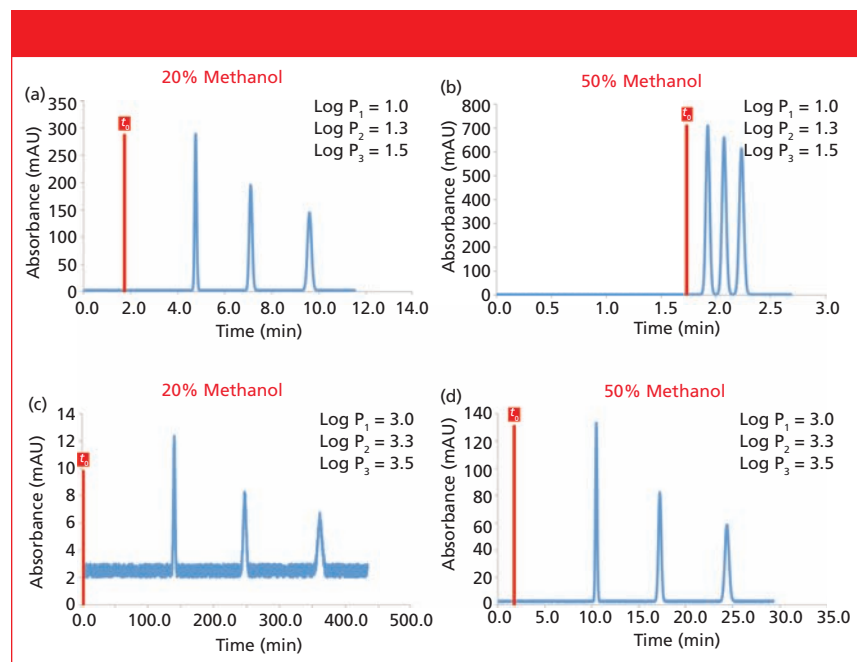


**Figure 5:** Practical chromatograms to demonstrate the impact of compound lipophilicity on retention in reversed-phase LC mode.

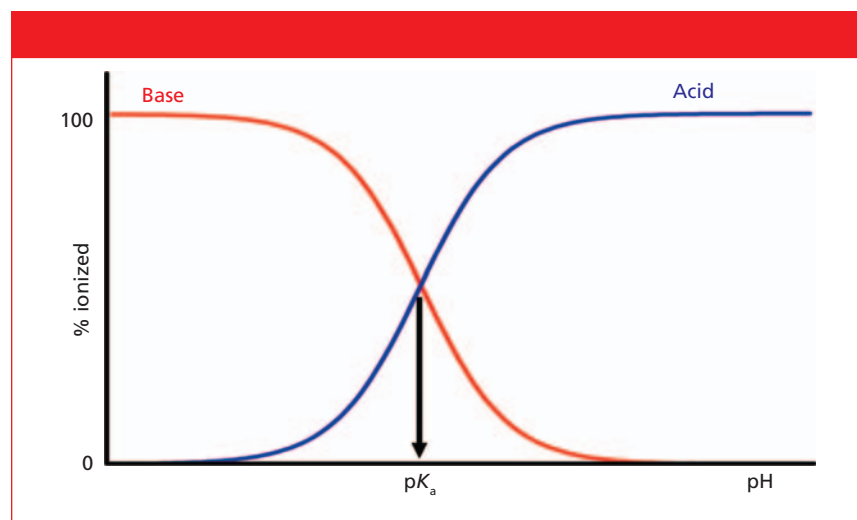


**Figure 6:** Impact of pH on the ionization state of acidic and basic substances.

was drawn, as well as the more practical curve representing  $N = f(F)$ .

### Using the “Efficiency” Spreadsheet

The user can modify the column dimensions ( $L_{col}$ ,  $d_{col}$ , and  $d_p$ ), as well as mobile-phase flow rate, to see the impact on a simulated chromatogram at the bottom of the spreadsheet. The corresponding plate count and column pressure drop are also calculated. In addition, users can visualize the corresponding van Deemter curve and evaluate whether the conditions are far from the optimal linear velocity (or flow rate). This ability to visualize the curve could help users determine the maximum plate count

achievable on the column under optimal flow rate conditions.

As shown in Figure 3a, an efficiency of 14,536 plates and a pressure drop of 38 bar were achieved on a 150 mm × 4.6 mm, 5- $\mu$ m  $d_p$  column at 1 mL/min, leading to a resolution greater than 1.5 for the chromatogram reported. Increasing the mobile-phase flow rate to 8 mL/min decreased the efficiency to only 5140 plates, which is in agreement with the van Deemter curve (see Figure 3b). The pressure drop also increased to 306 bar, as expected from Darcy’s law (equation 9). Next, the impact of particle size was illustrated in Figure 3c, where the efficiency was drastically improved ( $N = 62,241$  plates)

when the particle size was reduced from 5 to 1  $\mu$ m, but the pressure became incompatible with regular HPLC systems (955 bar). In Figure 3d, the column length was 50 mm and the particle size was 10  $\mu$ m. Compared to the chromatogram reported in Figure 3a, the last two peaks were not baseline resolved because of the poor efficiency (only 1807 plates), which is in agreement with equations 3 and 7. However, with such a short column, the pressure drop was only 3 bar.

## Understanding Retention in Reversed-Phase LC

### Theoretical Background

In reversed-phase LC mode, the retention at the surface of the alkyl stationary phase (for example, C18) is related to compound hydrophobicity and is often expressed as the partition coefficient ( $P$ ).  $P$  can be defined as the ratio of the compound concentrations between two immiscible phases (1-octanol and water) at equilibrium. For reasonable partition coefficient values (within a limited range), the logarithm of  $P$  should be considered ( $\log P$ ), and its definition is provided below:

$$\log P = \log \left( \frac{C_{\text{octanol}}}{C_{\text{aqueous}}} \right) \quad [10]$$

As illustrated in Figure 4, when the  $\log P$  value is less than 0, molecules are considered hydrophilic. Then, the molecule has greater affinity for the hydrophilic mobile phase versus the hydrophobic stationary phase and will therefore be poorly retained. In contrast, when the  $\log P$  value is greater than 0, the molecule is lipophilic and preferably interacts with the hydrophobic stationary phase, leading to significant retention. A few examples of hydrophilic and lipophilic molecules are given in Figure 4. In regular reversed-phase LC mode (with a C18 stationary phase and acetonitrile–water mobile phase), only compounds with  $\log P$  values between -1 and +6 can be adequately analyzed.

A simulated chromatogram with three compounds with different  $\log P$  values (set by the user) illustrates the chromatographic behavior for any mobile-phase composition (methanol percentage). For this spreadsheet, the transformation of  $\log P$  values into retention times was performed based on the work by Henchoz and colleagues (10), considering a Waters Acquity BEH Shield C18 column and a mobile phase containing methanol and water.

The following empirical equation was

used to calculate  $\log k_w$  (the extrapolated retention factor to pure water, mimicking 1-octanol–water partitioning [11]) based on the  $\log P$  value set by the user (10):

$$\log k_w = 0.83 \times \log P + 0.21 \quad [11]$$

Then,  $\log k_w$  was transformed into  $\log k$  at the mobile-phase composition set by the user using the following equation (12):

$$\log k = \log k_w - S\Phi \quad [12]$$

where  $\Phi$  is the volume fraction of the organic solvent (value between 0 and 1) and  $S$  is a characteristic constant for each solute, which corresponds to the elution strength of the organic modifier (slope of the logarithmic plot:  $d(\log k)/d\Phi$ ). In reversed-phase LC, the  $S$  value varies from approximately 3 (compounds of approximately 100 g/mol) to more than 100 for very large proteins. In this spreadsheet, a generic value of  $S = 4$  was considered because it is representative of low-molecular-weight compounds (<300 g/mol). Finally, the  $\log k$  values were transformed into  $t_R$  to construct the final chromatogram, considering the column dead time of a 150 mm  $\times$  4.6 mm, 5- $\mu$ m column

at a flow rate of 1 mL/min (column dead time of 1.74 min).

### Using the $\log P$ Spreadsheet

The user can modify the  $\log P$  values of three compounds to see the impact on the retention on a simulated chromatogram. In addition, users also have the ability to tune the mobile-phase composition by adjusting the methanol percentage.

As shown in Figure 5a, when the  $\log P$  values of the three compounds are between 1 and 1.5, 20% methanol is sufficient to elute all the peaks from the column within a reasonable analysis time of less than 10 min ( $k$  values between 1.5 and 4.5). This is because such compounds are not highly lipophilic (intermediate  $\log P$  values). To speed up the separation, Figure 5b shows that the same compounds can be eluted in less than 2.5 min when the mobile-phase composition is increased to 50% methanol. However, under these conditions, the retention was rather low because 50% methanol was too strong of an eluent ( $k$  values between 0.1 and 0.3). In Figure 5c, the compound lipophilicity ( $\log P$ ) was increased in the range of 3.0–3.5. When increasing the

$\log P$  values by only 2 units, the retention became much higher than Figure 5a and the analysis time was 360 min. To achieve a more reasonable analysis time with these lipophilic compounds, the mobile-phase composition was changed to 50% methanol, and these conditions allow the elution of all three compounds within 25 min.

The examples reported in Figure 5 demonstrate the benefits of reversed-phase LC, which can address a wide range of compound lipophilicity using a generic C18 material and simply adjusting the proportion of organic modifier in the mobile phase. If compounds with more diverse lipophilicity have to be analyzed, the isocratic mode would not be valid and gradient elution is used.

### Understanding the Impact of Compound Ionization in Reversed-Phase LC Theoretical Background

An important parameter for tuning retention and selectivity in reversed-phase LC is the mobile-phase pH. When considering ionizable substances (either acidic or basic), the pH impacts the percentage of neutral and ionized forms. Figure 6 shows the per-

## What Does the Future Hold for Ambient Air Monitoring Regulations?

### A PAMS Site Instrumentation Evaluation for VOC Monitoring

**ON-DEMAND WEBCAST** Aired September 28, 2016  
Register free at: [www.chromatographyonline.com/lcgc/air](http://www.chromatographyonline.com/lcgc/air)

The 1990 Clean Air Act Amendments (CAAA) required the promulgation of rules for enhanced monitoring of ozone, oxides of nitrogen (NOx), and volatile organic compounds (VOC) to obtain a more comprehensive and representative data on ozone air pollution. Subsequent regulations required states to establish Photochemical Assessment Monitoring Stations (PAMS) in ozone non-attainment areas classified as serious, severe, or extreme. The EPA recently commissioned an evaluation of current instrumentation to be used at future sites including the auto GC's used to measure VOC content in ambient air. In this webinar we will discuss the data and observations from the evaluation of the combined solution from Markes International and Thermo Scientific during this 2 year study. We will also review the use of this system in a newly initiated project for online VOC and semivolatle organic compounds (SVOC) monitoring surrounding oil well sites in collaboration with the Colorado Department of Public Health and Environment. Please join us.

#### Key Learning Objectives

- Review current objectives and regulation for ambient air monitoring at PAMS sites
- Explore current approaches to online air analysis for VOC ozone precursors
- Discuss the results of the EPA's technology evaluation for future PAMS sites
- Discover new strategies for VOC and SVOC monitoring in ambient air

#### Presenters

**Greg Harshfield**, Continuous Monitoring and Data Systems Supervisor, CDPHE

**Nicola Watson**, Sales Support Manager – Americas, Markes International

**Dwain Cardona**, Environmental Vertical Marketing Manager, Thermo Scientific

Moderator:

**Laura Bush**, Editorial Director, LCGC

#### Who Should Attend

- Anyone interested in learning more about online air monitoring for VOCs Contract laboratories who want to offer air analysis services to customers
- PAMS site personnel
- Environmental consultants who advise on sampling strategies
- Regulatory bodies who want to learn more about sampler types for VOCs and methodology
- Environmental lab organic bench chemists, lab managers and analysts

Sponsored by

**ThermoFisher**  
SCIENTIFIC

Presented by

**LCGC**

All attendees will receive a  
FREE executive summary  
of this webcast!

For questions, contact Kristen Moore at [kristen.moore@ubm.com](mailto:kristen.moore@ubm.com)



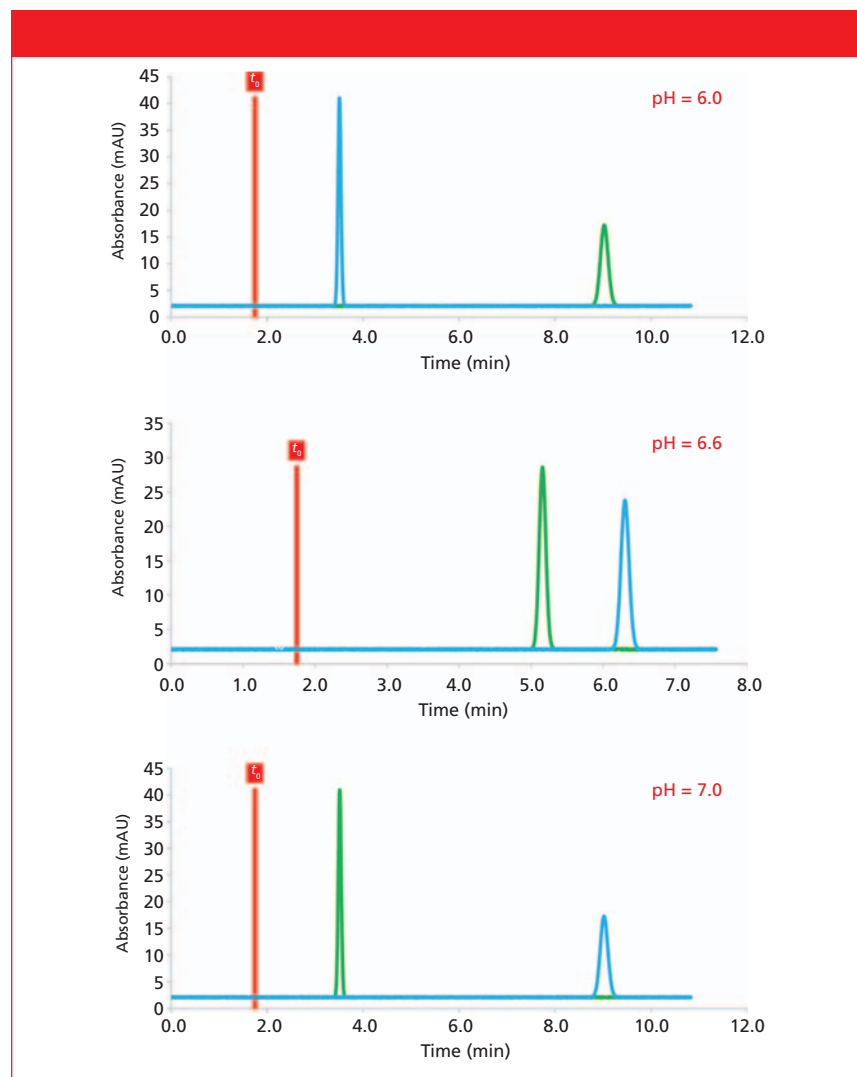


**Figure 7:** Impact of the mobile-phase pH and compound  $pK_a$  on retention in reversed-phase LC mode. The green peak corresponds to an acidic compound with a  $\log P$  of 2 and  $pK_a$  of 6.0, while the blue peak corresponds to a basic compound with a  $\log P$  of 2 and  $pK_a$  of 7.0. The experiments were performed at 25% methanol and only the pH was varied.

centages of the ionized form for an acidic (blue sigmoidal curve) and a basic substance (red sigmoidal curve) depending on the buffer pH and analyte  $pK_a$ .

Based on Figure 6, the retention of basic compounds decreases in reversed-phase LC at low pH (pH below the  $pK_a$  of the molecule) because of the presence of a high amount of ionized form. In contrast, the retention of acidic compounds increases in reversed-phase LC at low pH (pH below the  $pK_a$  of the molecule) because of the presence of a high proportion of neutral form. Ionized compounds are much more hydrophilic than neutral compounds; therefore, the retention and selectivity can be altered by tuning the mobile-phase pH. In the case of ionizable substances, the partition coefficient ( $\log P$ ) cannot be used and should be

replaced by the distribution coefficient ( $\log D$ ) expressed using the following equation for an acid (13):

$$\log D = \log \left( \frac{[AH]_{\text{octanol}}}{[A^-]_{\text{aqueous}} + [AH]_{\text{aqueous}}} \right) \quad [13]$$

For an acid, the percentages of neutral and ionized forms at a given pH are given by the following equations (14):

$$\%_{\text{ionized}} = \frac{100}{1 + 10^{pK_a - \text{pH}}} \quad [14]$$

$$\%_{\text{neutral}} = \frac{100}{1 + 10^{\text{pH} - pK_a}} \quad [15]$$

For a base, the percentages of neutral and ionized forms at a given pH are given by the following equations (14):

$$\%_{\text{ionized}} = \frac{100}{1 + 10^{\text{pH} - pK_a}} \quad [16]$$

$$\%_{\text{neutral}} = \frac{100}{1 + 10^{pK_a - \text{pH}}} \quad [17]$$

All the calculations were made for a 150 mm  $\times$  4.6 mm, 5- $\mu\text{m}$  column at a flow rate of 1 mL/min using methanol as the organic modifier. Only two compounds were selected for the simulation to limit the complexity of the sample, and a color code was used to distinguish the two substances. For these two compounds, the user can set the  $\log P$  and  $pK_a$  values, as well as the nature of the compound (acidic or basic). In addition, the user also has to define the mobile-phase pH and the percentage of methanol in the mobile phase. Based on these inputs, the  $\log D$  at the pH indicated by the user is calculated using the following two equations for an acid (equation 18) or a base (equation 19) (13):

$$\log D = \log P - \log(1 + 10^{\text{pH} - pK_a}) \quad [18]$$

$$\log D = \log P - \log(1 + 10^{pK_a - \text{pH}}) \quad [19]$$

For  $(\text{pH} - pK_a)$  values greater than  $|3.5|$ ,  $\log D$  was constant. The  $\log D$  values were then transformed into retention factors using equations 11 and 12.

The impact of the mobile-phase pH and compound  $pK_a$  can be directly visualized. In addition to the simulated chromatogram, the ionization profiles of the two simulated compounds are presented in the upper part of the spreadsheet.

### Using the $pK_a$ Spreadsheet

Figure 7 illustrates the impact of the mobile-phase pH (modified in a very narrow range around the  $pK_a$  of the substances) on the chromatographic separation of two species (one acid and one base) with identical  $\log P$  values. The retention of the acid (green peak) decreases with pH, which is logical because the acid is mostly deprotonated at higher pH (charged compounds are less retained in reversed-phase LC mode). In contrast, the retention of the base (blue peak) increases with pH because the molecules are less charged at a higher pH. Because the mobile-phase pH was very close to the  $pK_a$  of the two substances, the impact of a pH change on retention was significant for both compounds. In these three examples, the elution order was completely reversed between pH 6.0 and 7.0.



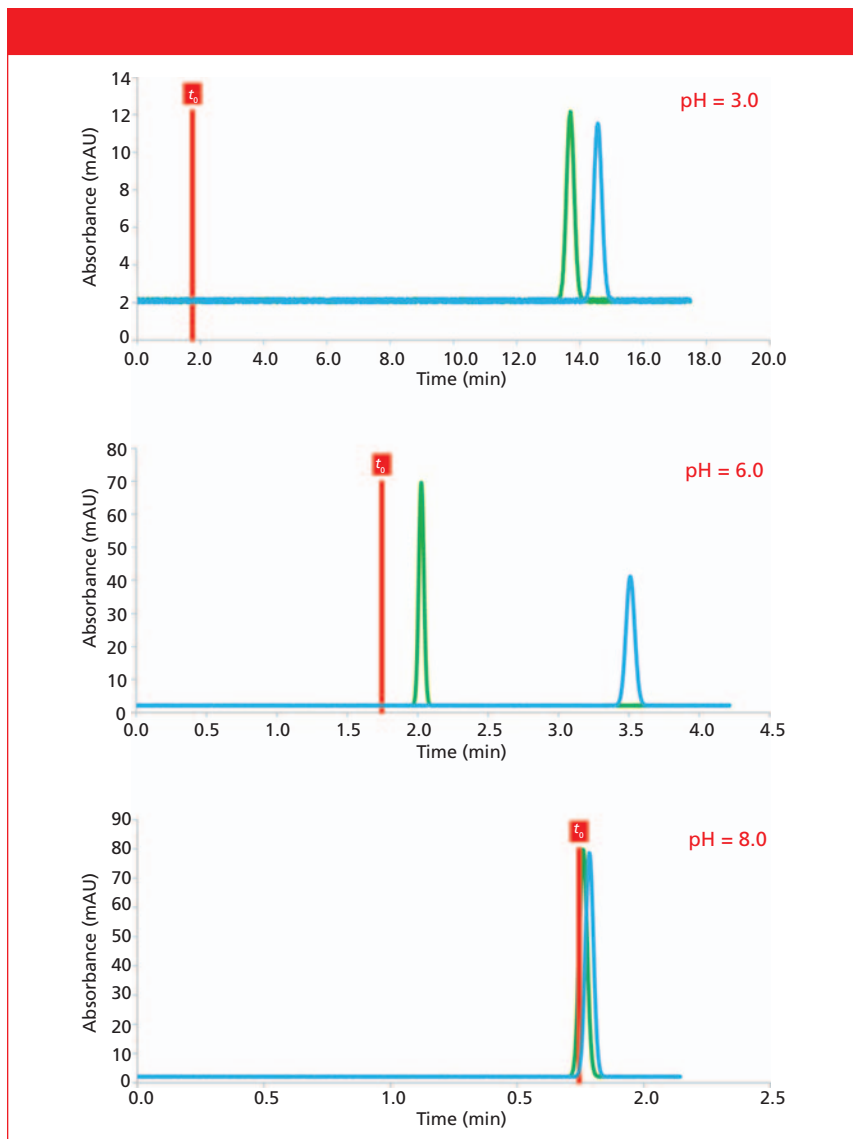


**Figure 8:** Impact of the mobile-phase pH and compound  $pK_a$  on retention in reversed-phase LC mode. The green peak corresponds to an acidic compound with a log  $P$  of 2 and  $pK_a$  of 4.0, while the blue peak corresponds to an acidic compound with a log  $P$  of 2 and  $pK_a$  of 5.0. The experiments were performed at 25% methanol and only the pH was varied.

In the second example (Figure 8), two acids were selected, and the pH was varied in a much wider range (from pH 3.0 to 8.0). The retention was significant at pH 3.0 for these two acidic molecules. The retention factor was approximately 8 on average, and the two peaks were just baseline resolved. When the pH was increased to 6.0, the retention decreased ( $k$  between 0.2 and 1.0), but the two peaks were much better resolved. Finally, at more basic pH (8.0), the peaks were not sufficiently retained and were not resolved. Under these conditions, the two acidic molecules were completely deprotonated and unsuitable for reversed-phase LC at 25% methanol. A lower proportion of methanol would improve the separation quality.

These examples illustrate the impact of the mobile-phase pH on retention, selectivity, and resolution in reversed-phase LC mode and the importance of adequately controlling this variable in reversed-phase LC.

### Conclusion

In conclusion, the spreadsheet HPLC Teaching Assistant (15) helps in learning and teaching liquid chromatography in an innovative and efficient way, using virtual (simulated) chromatograms obtained under numerous analytical conditions. This tool can be used by academic teachers, as well as company training instructors, who are interested in using innovative technology to better convey information during their courses.

### Acknowledgments

The authors wish to thank Dr. Szabolcs Fekete from the University of Geneva for his critical review of the manuscript and his suggestions to improve the spreadsheet.

### References

- (1) I. Molnar, *J. Chromatogr. A* **965**, 175–194 (2002).
- (2) E.F. Hewitt, P. Lukulay, and S. Galushko, *J. Chromatogr. A* **1107**, 79–87 (2006).
- (3) S. Heinisch and J.L. Rocca, *Chromatographia* **32**, 559–565 (1991).
- (4) R.C. Rittenhouse, *J. Chem. Educ.* **72**, 1086 (1995).
- (5) I.C. Bowater and I.G. McWilliam, *J. Chem. Educ.* **71**, 674–678 (1994).
- (6) R.A. Shalliker, S. Kayillo, and G.R. Dennis, *J. Chem. Educ.* **85**, 1265–1268 (2008).
- (7) J.C. Reijenga, *J. Chromatogr. A* **903**, 41–48 (2000).
- (8) P.G. Boswell, D.R. Stoll, P.W. Carr, M.L. Nagel, M.F. Vitha, and G.A. Mabbott, *J. Chem. Educ.* **90**, 198–202 (2013).
- (9) J. Li and P.W. Carr, *Anal. Chem.* **69**, 2550–2553 (1997).
- (10) Y. Henchoz, D. Guillarme, S. Martel, S. Rudaz, J.L. Veuthey, and P.A. Carrupt, *Anal. Bioanal. Chem.* **394**, 1919–1930 (2009).
- (11) D. Benhaim and E. Grushka, *J. Chromatogr. A* **1217**, 65–74 (2010).
- (12) S. Martel, D. Guillarme, Y. Henchoz, A. Galland, J.L. Veuthey, S. Rudaz, and P.A. Carrupt, in *Molecular Drug Properties: Measurement and Prediction*, Volume 37, R. Mannhold, Ed. (Wiley-VCH, 2008), pp. 331–355.
- (13) R.A. Scherrer and S.M. Howard, *J. Med. Chem.* **20**, 53–58 (1977).
- (14) H.N. Po and N.M. Senozan, *J. Chem. Educ.* **78**, 1499–1503 (2001).
- (15) This spreadsheet can be downloaded for free at: [https://epgl.unige.ch/labs/fanal/hplc\\_teaching/en](https://epgl.unige.ch/labs/fanal/hplc_teaching/en).

**Davy Guillarme and Jean-Luc Veuthey** are with the School of Pharmaceutical Sciences at the University of Geneva, University of Lausanne in Geneva, Switzerland.

Direct correspondence to: [davy.guillarme@unige.ch](mailto:davy.guillarme@unige.ch) ■

For more information on this topic,  
please visit  
[www.chromatographyonline.com](http://www.chromatographyonline.com)